Science Advances
AAAS

advances.sciencemag.org/cgi/content/full/6/44/eaba0682/DC1

# Supplementary Materials for

## Genome integrity and neurogenesis of postnatal hippocampal neural stem/progenitor cells require a unique regulator Filia

Jingzheng Li, Yafang Shang, Lin Wang, Bo Zhao, Chunli Sun, Jiali Li, Siling Liu, Cong Li, Min Tang, Fei-Long Meng*, Ping Zheng*

*Corresponding author. Email: zhengp@mail.kiz.ac.cn (P.Z.); feilong.meng@sibcb.ac.cn (F.-L.M.)

Published 28 October 2020, *Sci. Adv.* **6**, eaba0682 (2020)
DOI: 10.1126/sciadv.aba0682

**The PDF file includes:**



**Other Supplementary Material for this manuscript includes the following:**

(available at advances.sciencemag.org/cgi/content/full/6/44/eaba0682/DC1)

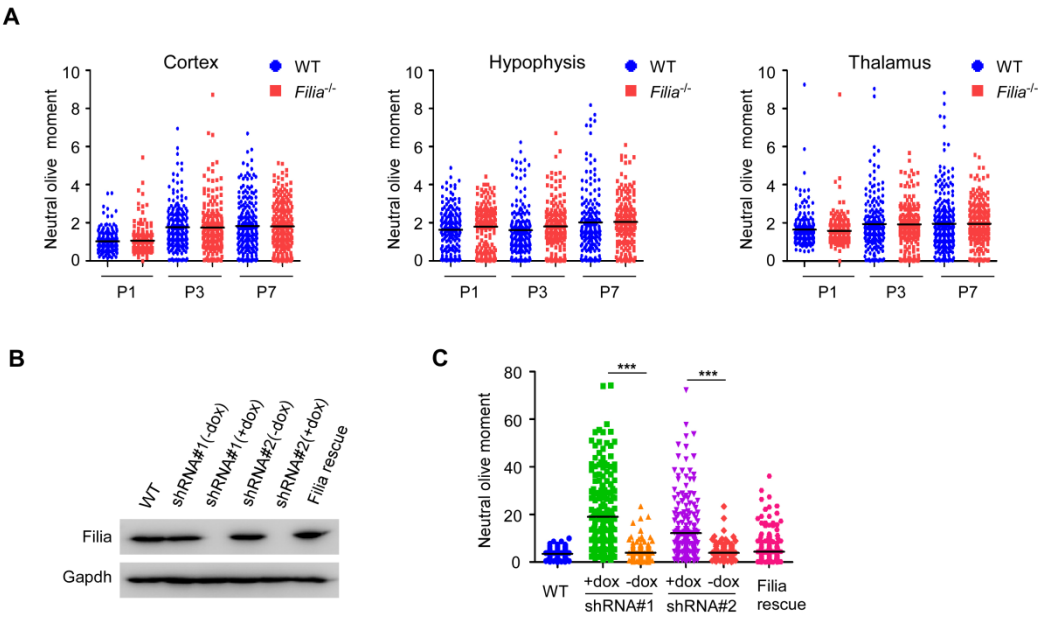


**Fig. S1**. **Filia maintains genomic stability of hippocampal cells after birth.**

(**A**) Filia depletion had no influence on the genome integrity of cells in regions of cortex, hypophysis, and thalamus when examined at postnatal day 1 (P1), P3 and P7 by neutral comet assay. (**B**) Efficient knockdown of Filia in cultured mouse NSPCs by two independent doxycycline (dox)-inducible shRNAs. Filia was re-expressed in knockdown cells. (**C**) Neutral comet assay showed that knockdown of Filia by two shRNAs significantly increased the DNA DSB levels in cultured mouse NSPCs. Re-expression of Filia rescued the defect. Data were represented as mean ± SEM; two-tailed Student's test; ***$P < 0.001$.

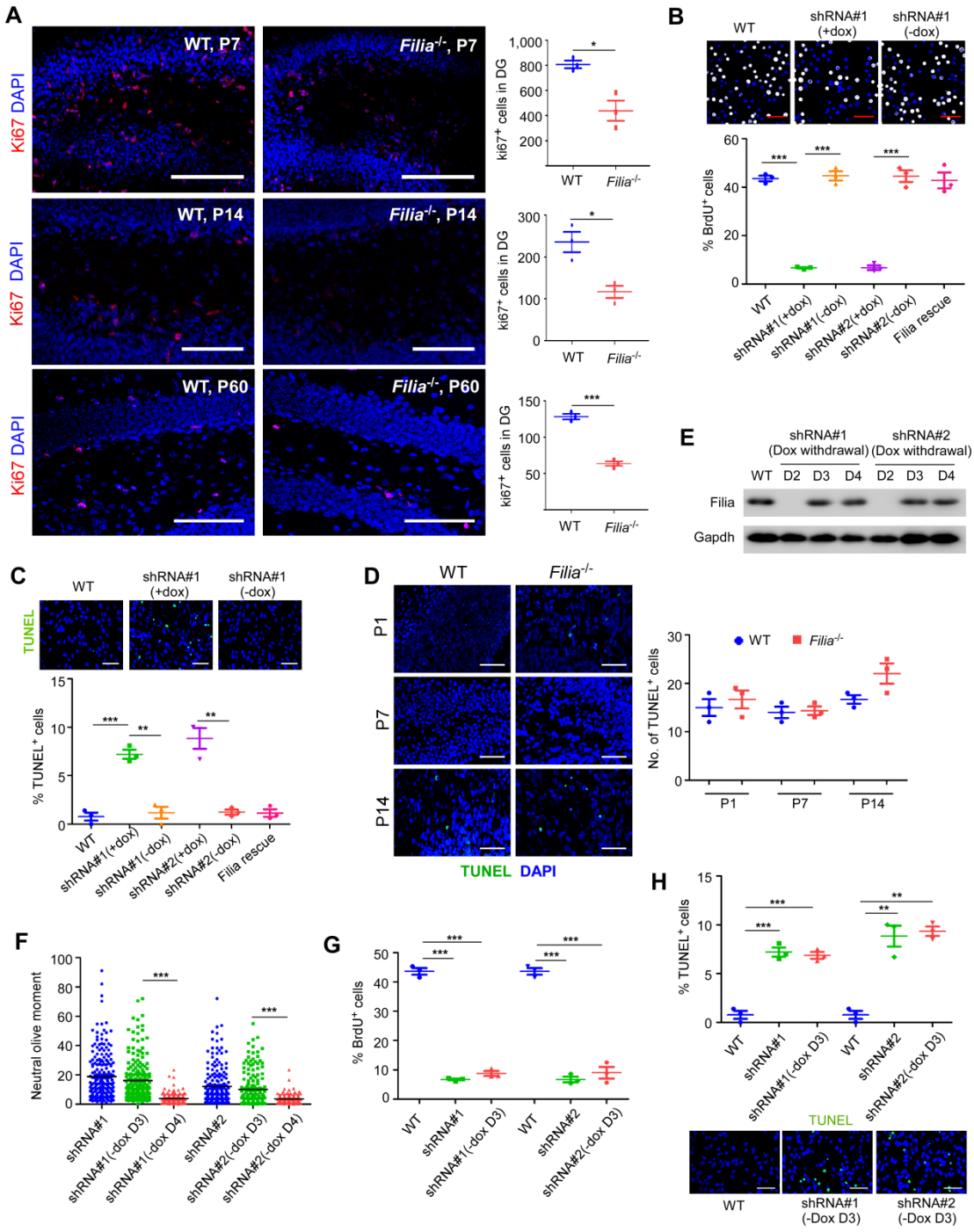


**Fig. S2. Filia depletion impairs the proliferation and induces apoptosis of cultured mouse NSPCs.**

(**A**) Filia loss impaired the *in vivo* proliferation of hippocampal NSPCs, as examined by Ki67 expression at P7, P14, and P60. Right panel showed the quantification of $Ki67^+$ cells in dentate gyrus (DG). Scale bar, 100 μm. (**B**) Knockdown of Filia in

cultured NSPCs by dox-inducible shRNAs decreased the proportions of dividing cells capable of BrdU incorporation. Re-expression of Filia rescued the defect. Scale bar, 50 μm. (**C**) Knockdown of Filia in cultured NSPCs by shRNAs increased the rates of apoptosis. Re-expression of Filia restored the cell viability. Scale bar, 50 μm. (**D**) TUNEL staining of brain sections showed that Filia depletion did not enhance cell apoptosis in hippocampus when examined at P1, P7 and P14. Scale bar, 100 μm. (**E**) In dox-induced Filia knockdown NSPCs, removal of dox could restore Filia expression at as early as day 3. (**F**) On day 3 of dox removal, although Filia expression was restored, the DNA DSBs persisted in cultured NSPCs. The proliferation (**G**) and apoptosis rates (**H**) of NSPCs were not rescued by re-expression of Filia on day 3 of dox removal. Scale bars in (H), 50 μm. Data were represented as mean ± SEM; two-tailed Student's test; $*P < 0.05$, $**P < 0.01$, $***P < 0.001$.

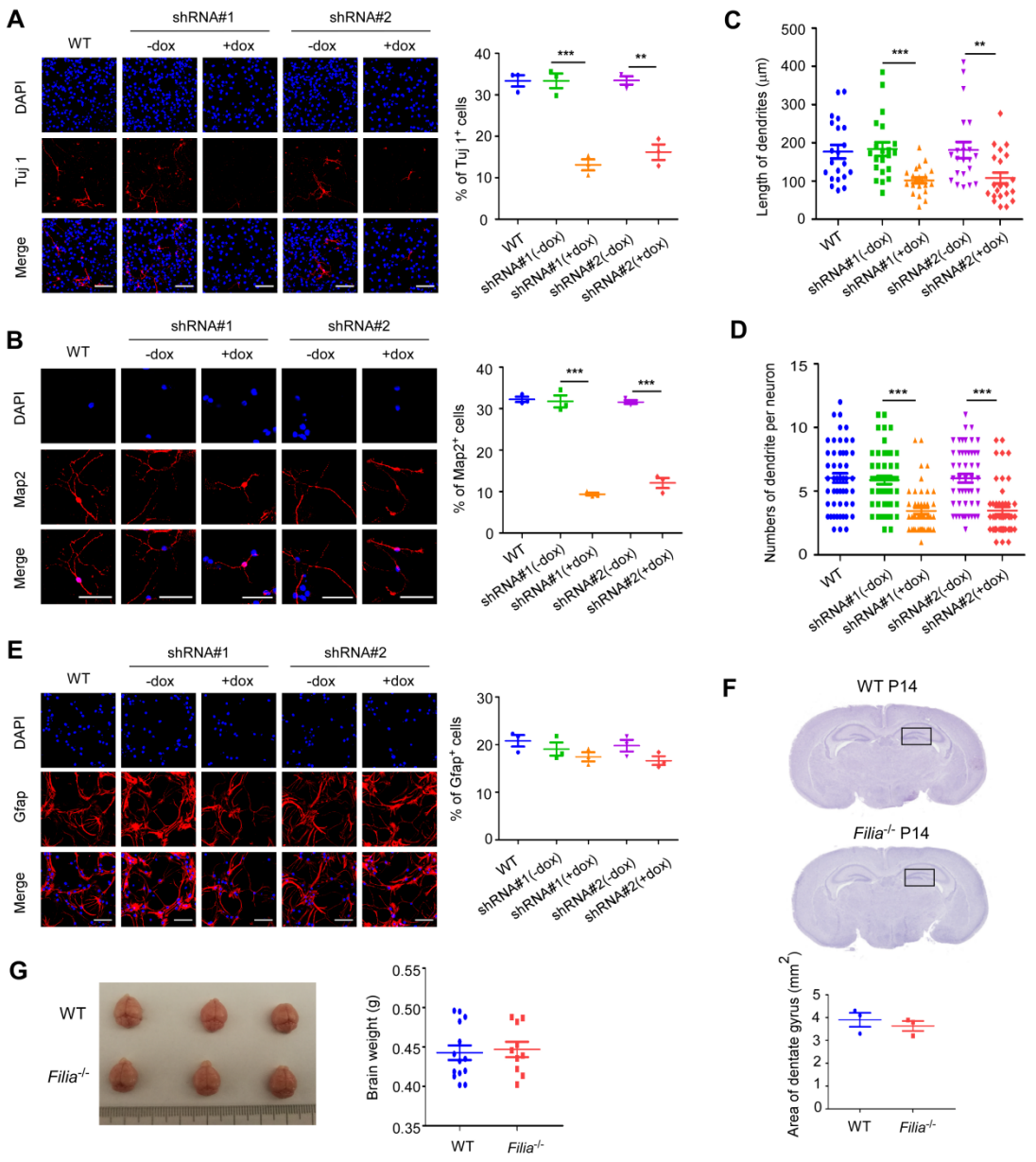


**Fig. S3. Filia deletion impairs hippocampal neurogenesis.**

*In vitro* differentiation assay showed that dox-induced Filia knockdown impaired the differentiation of cultured NSPCs into immature neurons (Tuj1$^+$ cells) (**A**) and mature neurons (Map2$^+$ cells) (**B**). The neurons differentiated from cultured NSPCs displayed reduced dendritic length (**C**) (*n* = 21 cells) and numbers (**D**) (*n* = 50 cells) when Filia was knocked down. (**E**) *In vitro* differentiation of NSPCs into astrocytes was not affected by Filia depletion. (**F**) The overall hippocampus size and structure were not

apparently affected by Filia depletion. (**G**) *Filia*$^{-/-}$ mice had normal brain structure and weights. Data were represented as mean ± SEM; two-tailed Student's test; $^{**}P < 0.01$, $^{***}P < 0.001$. Scale bars in A, B and E, 50 μm. Credit for photo in S3G: Jingzheng Li, Kunming Institute of zoology, Chinese Academy of Sciences.

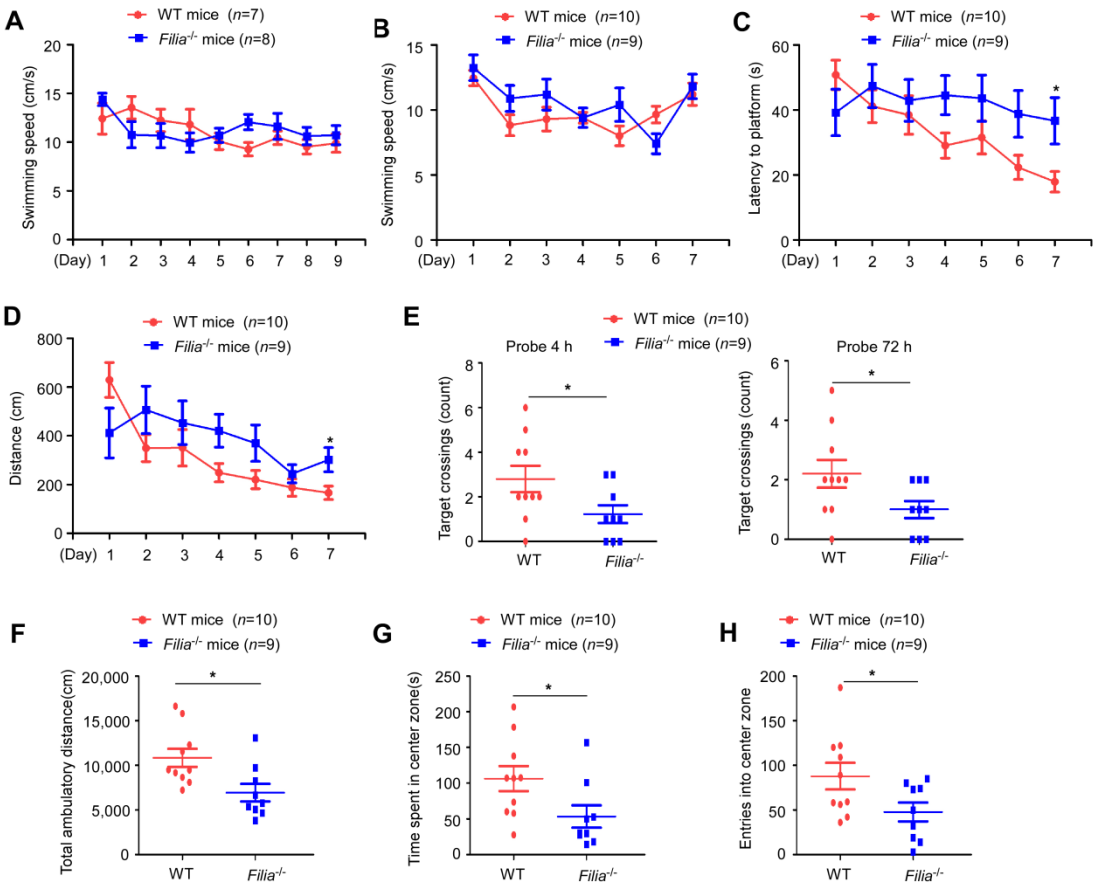


**Fig. S4. Filia depletion impairs hippocampal functions in learning, memory and emotional regulation.**

*Filia*$^{-/-}$ and WT mice swam in similar speeds at two-month (**A**) and one-year old (**B**). Morris water maze test was performed on one-year old mice. *Filia*$^{-/-}$ mice spent more time (**C**) and traveled longer distance (**D**) in locating the platform at the 7$^{th}$ day of training. At 4 h and 72 h of probe trials, *Filia*$^{-/-}$ mice showed fewer platform crossings than WT littermates (**E**). In open field test performed on one-year old mice, *Filia*$^{-/-}$ mice showed weaker locomotivity (**F**), spent much less time in the center zone (**G**), and exhibited fewer entries into the center zone (**H**). Data were represented as mean ± SEM; two-way ANOVA with Bonferroni post hoc test (A-D); two-tailed Student's test (E-H); *$P < 0.05$.

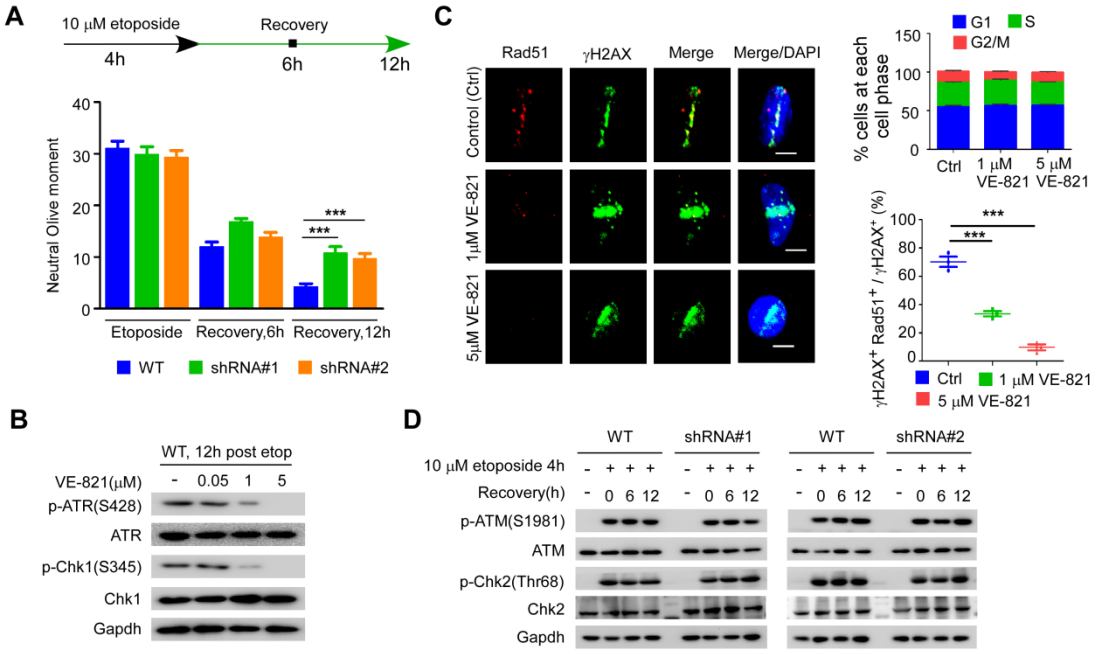


**Fig. S5. Filia-ATR axis regulates the HR repair pathway.**

(**A**) Neutral comet assay showed Filia dysfunctions compromised DNA DSB repair. (**B**) ATR activation was successfully blocked by specific inhibitor VE-821 in a dose-dependent manner during response to DNA DSBs. (**C**) Blockage of ATR activation by VE-821 significantly suppressed the recruitment of Rad51 to DNA DSB sites labeled with γH2AX in a dose-dependent manner. Because the cell cycle was not altered by temporary inhibition of ATR, the decreased proportions of $\gamma H2AX^{+}Rad51^{+}$ cells among $\gamma H2AX^{+}$ cells reflected impairment of HR repair. 50 cells were examined in one replicate and total three repeats were performed. (**D**) The activation of ATM and Chk2 in Filia knockdown NSPCs was as normal as in WT counterparts. Data were represented as mean ± SEM; one-way ANOVA with Bonferroni post hoc test; ***$P < 0.001$; scale bar, 5 μm.

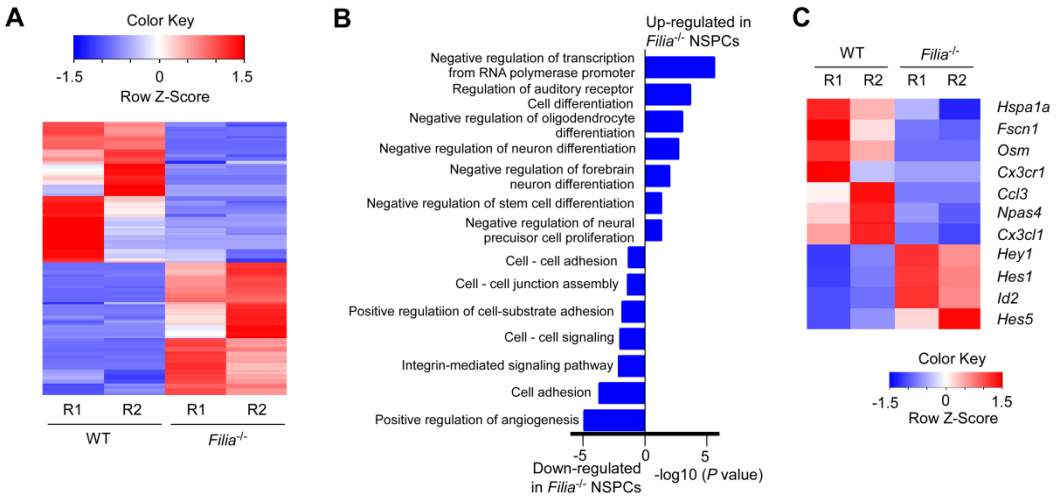


**Fig. S6. RNA sequencing analysis of hippocampal NSPCs in WT and *Filia*$^{-/-}$ mice.**

(**A**) 169 differentially expressed genes (DEGs) were identified in hippocampal NSPCs between WT and *Filia*$^{-/-}$ mice. Data were from two replicates (R1 and R2). (**B**) Gene ontology (GO) enrichment analysis of DEGs in hippocampal NSPCs between WT and *Filia*$^{-/-}$ mice. (**C**) Expression patterns of several example genes crucial for neurogenesis.

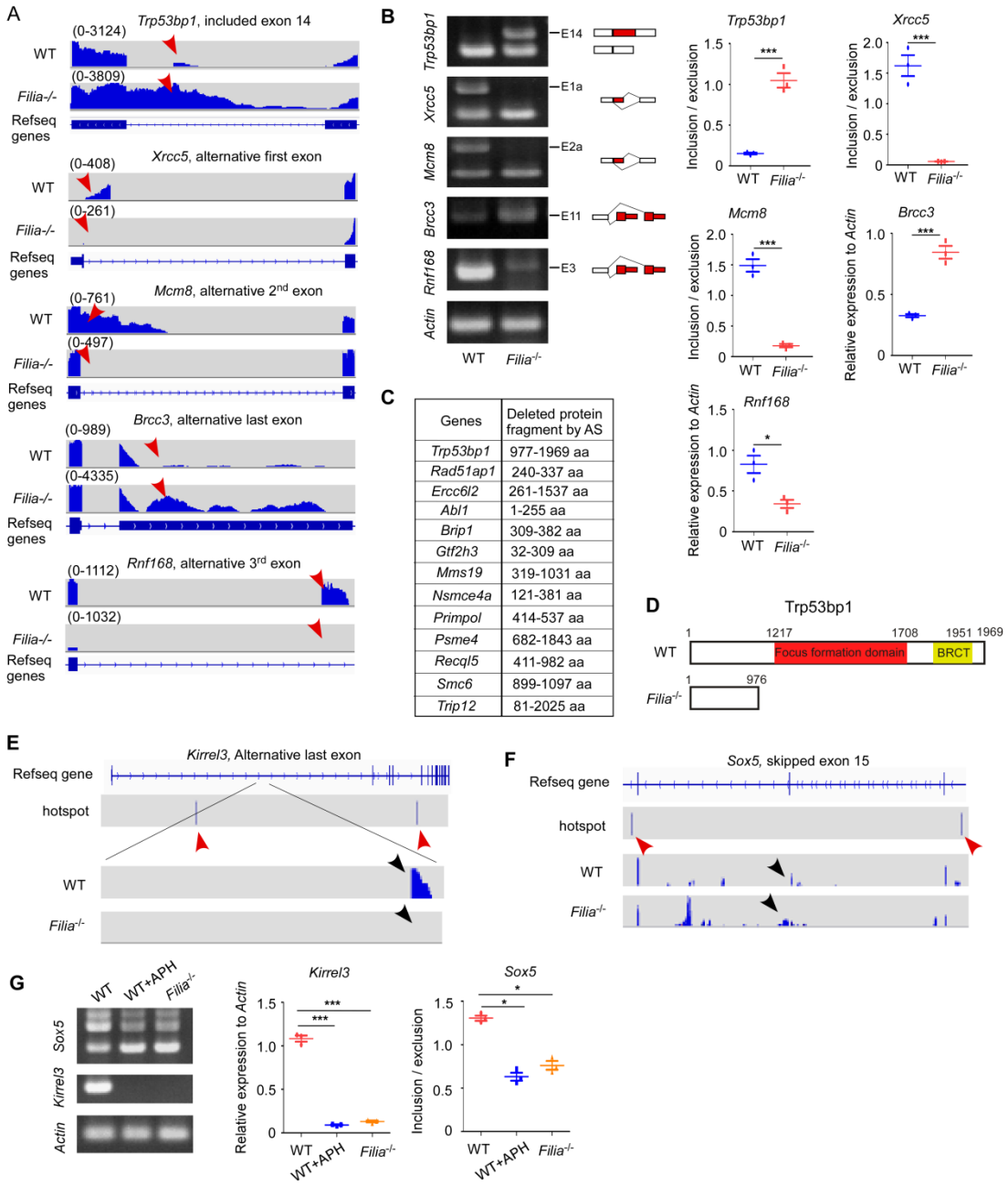


**Fig. S7. Examples of several genes with alternative splicing in *Filia*$^{-/-}$ hippocampal NSPCs.**

(**A**) Examples of five genes with alternative splicing in *Filia*$^{-/-}$ NSPCs. Alternative splicing was visualized using IGV software. Alternative exons were indicated by red arrows. The numbers on the left indicated the sites of exons. (**B**) Validation of alternative splicing of five genes by semi-quantitative RT-PCR. Right panel showed

the quantifications of isoform expressions from three replications. E is short for exon. (**C**) Genes whose alternative splicing (AS) in *Filia*$^{-/-}$ NSPCs was predicted to cause obvious protein fragment deletion. aa is short for amino acid. (**D**) Diagrams showing Trp53BP1 protein change in *Filia*$^{-/-}$ NSPCs. In RDC genes *Kirrel3* (**E**) and *Sox5* (**F**), an exon present in WT NSPCs but absent in *Filia*$^{-/-}$ cells was flanked by DSBs. Red arrowheads indicate DSBs and black arrowheads indicate alternatively spliced exons. (**G**) Semi-quantitative RT-PCR showed that the alternative splicing of *Kirrel3* and *Sox5* in *Filia*$^{-/-}$ NSPCs was similar to that in WT NSPCs treated with aphidicolin. Right panel showed the quantifications of isoform expressions from three replications. Data were represented as mean ± SEM; two-tailed Student's test; **P* < 0.05, ****P* < 0.001.

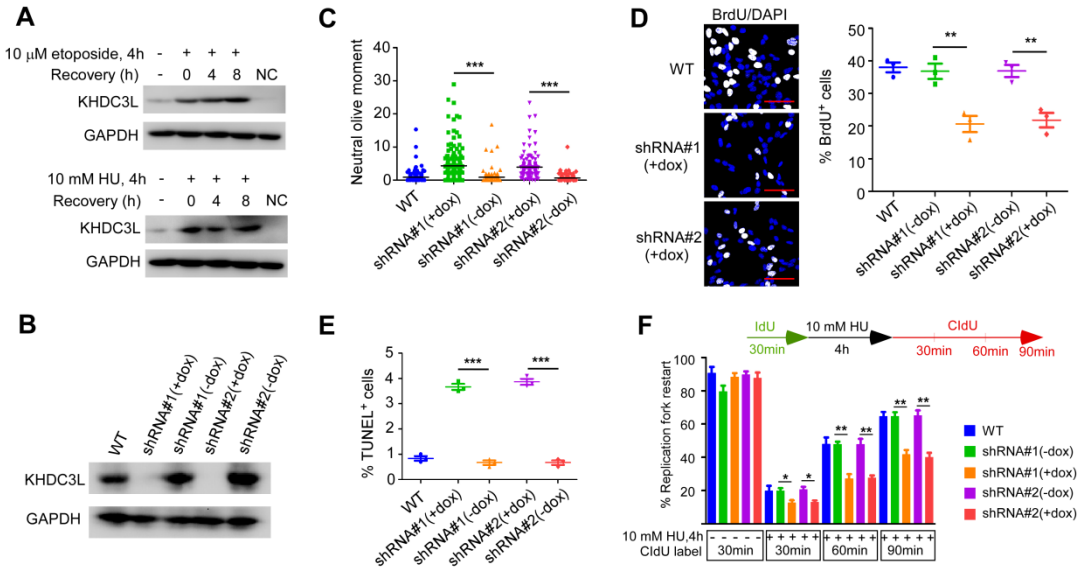


**Fig. S8. Primate ortholog KHDC3L is expressed in cultured rhesus monkey NSPCs and regulates genomic stability.**

(**A**) KHDC3L protein was expressed in cultured rhesus monkey NSPCs and genotoxic insults (etoposide or HU treatment) stimulated the expression. (**B**) KHDC3L was efficiently knocked down in monkey NSPCs by two independent dox-inducible shRNAs. (**C**) Neutral comet assay showed that KHDC3L depletion caused significant increase in DNA DSB levels in cultured monkey NSPCs. (**D**) BrdU incorporation assay and FACS analysis revealed that KHDC3L depletion compromised the proliferation of monkey NSPCs. Scale bar, 50 μm. (**E**) TUNEL staining and FACS analysis showed the elevated apoptosis of monkey NSPCs depleted of KHDC3L. (**F**) DNA fiber assay indicated that KHDC3L knockdown decreased the rates of stalled fork restart in monkey NSPCs. Data were represented as mean ± SEM; two-tailed Student's test; **P* < 0.05, ***P* < 0.01, ****P* < 0.001.

**Table S1. Primers used in this study.**

| Gene | | Primers |
|---|---|---|
| Quantitative real time-PCR | | |
| *Filia* | Forward | 5'-GGTGAAACGGGTACACTATGG -3' |
| | Reverse | 5’-CCACGTACAGTCTTTTTGGATCT-3' |
| *Actin* | Forward | 5’-TTGCTGATCCACATCTGCTGGAAGG-3' |
| | Reverse | 5’-GTGTGACGTTGACATCCGTAAAGAC-3' |
| Single cell RT-PCR | | |
| *Nestin* | Forward | 5’-TAACTGCCCTAGAGACGGTGT-3' |
| | Reverse | 5’-AGATGCACAGGAGACCCTACTA-3' |
| *Filia* | Forward | 5’-TGGAAATCATGTTTGGTAAGGA-3' |
| | Reverse | 5’-CCATACGACGACGCTCAACT-3' |
| *Neun* | Forward | 5'-AGTCCACGTCTGGCGTACAC-3' |
| | Reverse | 5’-AGACCTGGGATGAGTGATAAGC-3' |
| *Gfap* | Forward | 5’-CCAAACTGGCTGATGTCTACC-3' |
| | Reverse | 5’-TTTCTCTCCAAATCCACACGA-3' |
| Alternative splicing | | |
| *Sox5* | Forward | 5’-GCAGCAACAACACAAAATCAACTT-3' |
| | Reverse | 5’-ATGCAGGTGATTTGCCATCAGA-3' |
| *Kirrel3* | Forward | 5’-CGGAGACACAACGAGACCTA-3' |
| | Reverse | 5’-GCTGTGAGAACATTTATGCCACT-3' |
| *Trp53bp1* | Forward | 5’-GGAGCCCAAGAGACATAGTAC-3' |
| | Reverse | 5’-AGTTGTAGGCTTTTCCAGGCTAA-3' |
| *Xrcc5* | Forward | 5’-CTGAGTTGCGACACTCTAGGTT-3' |
| | Reverse | 5’-GATTCTTCACCAGGAAAGGAGT-3' |
| *Brcc3* | Forward | 5’-TCTTCCCTAGAATAAAGCATGAG-3' |
| | Reverse | 5’-CTTGTGGAGGTTCAATGCGTTG-3' |
| *Mcm8* | Forward | 5’-AGCCTCACAACCGTTACTTCAAC-3' |
| | Reverse | 5’-CCACCAAAATGCTTCCTTTTCTT-3' |
| *Rnf168* | Forward | 5’-GTCTCTTCGTGGACTCGGTAC-3' |
| | Reverse | 5’-AGGTGGGTGTTCACGGATTAGC-3' |
| 3’ UTR shRNA sequence | | |
| *Filia* | shRNA#1 | 5’-ACGTCTGCAAATCCAGAACCTA-3' |
| | shRNA#2 | 5’-GAGTAAGGCAATGATCTTAAAC-3' |
| *KHDC3L* | shRNA#1 | 5’-CTTCTGTTGAATGGTTGCAAAC-3' |
| | shRNA#2 | 5’-CAAACACAAACTTGAGTTCTAA-3' |
| Mouse genotyping | | |
| *GFP* | Forward | 5’-GAGCTGGACGGCGACGTAAAC-3’ |
| | Reverse | 5’-CGTTGTGGCTGT TGTTAGTTGTAC-3’ |
| *Filia* | P1 | 5’-TGCCTGGGCAGGTTATTTAG-3’ |
| | P2 | 5’-CGAGCGTCTGAAACCTCTTC-3’ |

| | | |
|---|---|---|
| | P3 | 5’-AGCTAGCTTGGCTGGACGTA-3’ |
| HTGTS | | |
| Chr12-sgRNA | sense | 5’-CACCATTCCGCCAACCCTCGAGAT-3' |
| | antisense | 5’-AAACATCTCGAGGGTTGGCGGAAT-3' |
| Chr15-Myc-sgRNA | sense | 5’-CACCGCCCTATTTCATCTGCGACG-3' |
| | antisense | 5’-AAACCGTCGCAGATGAAATAGGGC-3' |
| Bio- Chr12-sgRNA | | Bio/CAGGTGCCAAGTTCTACCAACAAGC |
| Chr12-sgRNA Red | | CCTCTAAGATAAAAACTGGAAGTAGTT |
| Bio-Chr15-Myc-sgRNA | | Bio/CGAGCGTCACTGATAGTAGGGAGT |
| Chr15-Myc-sgRNA Red | | GCACCAACCAGAGCTGGATAACTCT |

**Table S2. Antibody information.**

| Name | Company | Catalog# | Clone# | Dilution |
|---|---|---|---|---|
| Mouse monoclonal anti-IdU | BD Biosciences | 347580 | B44 | 1:500 (IF) |
| Rat monoclonal anti-BrdU, also used for immunostaining of CIdU | Novus | NB500-169 | BU1/75 | 1:1000(IF) |
| Rabbit polyclonal anti-Gfap | Abcam | ab7260 | | 1:1000(IF) |
| Rabbit monoclonal anti-NeuN | Abcam | ab177487 | EPR12763 | 1:2000(IF) |
| Rabbit monoclonal anti-ki67 | Abcam | ab16667 | SP6 | 1:300(IF) |
| Mouse monoclonal anti-Pcna | Cell Signaling Technology | 2586S | PC10 | 1:1000(IF) |
| Mouse monoclonal anti-Tuj1 | Abcam | ab78078 | 2G10 | 1:200(IF) |
| Rabbit monoclonal anti-Map2 | Millipore | AB5622 | | 1:300(IF) |
| Mouse monoclonal anti-Gapdh | Sangon Biotech | D190090 | | 1:1000(IB) |
| Rabbit polyclonal anti-Histone H2B | EnoGene | E1A0866 | | 1:1000(IB) |
| Rabbit polyclonal anti-γ-H2AX | Cell Signaling Technology | 9718 | 20E3 | 1:500(IF) |
| Mouse anti-Rad51 antibody | Abnova | H00005888-B01P | | 1:500(IF) |
| Rabbit anti-p-ATR (Ser428) | Cell Signaling Technology | 2853S | | 1:1000(IB) |
| Rabbit polyclonal anti-ATR | Cell Signaling Technology | 2790S | | 1:1000(IB) |
| Mouse monoclonal anti-p-ATM(Ser1981) | Novus | NB100-307 | 10H11.E12 | 1:1000(IB) |
| Rabbit monoclonal anti-ATM | Cell Signaling Technology | 2873S | D2E2 | 1:1000(IB) |
| Mouse monoclonal anti- Chk1 | Cell Signaling Technology | 2360S | 261D5 | 1:1000(IB) |
| Rabbit monoclonal anti-Chk2 | Cell Signaling Technology | 2662S | | 1:1000(IB) |
| Rabbit monoclonal anti-P-Chk1(S345) | Cell Signaling Technology | 2348S | 133D3 | 1:1000(IB) |
| Rabbit monoclonal anti-P-Chk2(Thr68) | Cell Signaling Technology | 2917S | C13C1 | 1:1000(IB) |
| Rabbit anti-KHDC3L antibody | Abcam | ab126339 | | 1:1000(IB) |
| Goat anti-Mouse IgG Secondary Antibody, Alexa Fluor 488 | Thermo Fisher Scientific | A11029 | | 1:500(IF) |
| Donkey anti-Mouse IgG Secondary Antibody, Alexa Fluor 555 | Thermo Fisher Scientific | A31570 | | 1:500(IF) |
| Goat anti-Rabbit IgG Secondary Antibody, Alexa Fluor 488 | Thermo Fisher Scientific | A11034 | | 1:500(IF) |
| Donkey anti-Rabbit IgG Secondary Antibody, Alexa Fluor 555 | Thermo Fisher Scientific | A31572 | | 1:500(IF) |

| | | | | |
|---|---|---|---|---|
| Goat anti-Rat IgG Secondary Antibody, Alexa Fluor Cy3 | Thermo Fisher Scientific | A10522 | | 1:500(IF) |
| Goat anti-Rat IgG Secondary Antibody, Alexa Fluor 647 | Thermo Fisher Scientific | A21247 | | 1:500(IF) |
| Goat anti-Mouse IgG (H+L) Secondary Antibody, HRP | Thermo Fisher Scientific | 31430 | | 1:5000(IB) |
| Goat anti-Rabbit IgG (H+L) Secondary Antibody, HRP | Thermo Fisher Scientific | 31460 | | 1:5000(IB) |